Check for updates

Received: 6 December 2021 | Revised: 21 December 2021 | Accepted: 23 December 2021

DOI: 10.1111/mmi.14876

RESEARCH ARTICLE

WILEY

BldD-based bimolecular fluorescence complementation for in vivo detection of the second messenger cyclic di-GMP

Manuel Halte[1] | Mirka E. Wörmann[2] | Maxim Bogisch[2] | Marc Erhardt[1,3] | Natalia Tschowri[4]

[1]Institute for Biology/Bacterial Physiology, Humboldt-Universität zu Berlin, Berlin, Germany

[2]Institute for Biology/Microbiology, Humboldt-Universität zu Berlin, Berlin, Germany

[3]Max Planck Unit for the Science of Pathogens, Berlin, Germany

[4]Institute for Microbiology, Leibniz Universität Hannover, Hannover, Germany

Correspondence
Marc Erhardt, Institute for Biology/Bacterial Physiology, Humboldt-Universität zu Berlin, 10115 Berlin, Germany.
Email: marc.erhardt@hu-berlin.de

Natalia Tschowri, Institute for Microbiology, Leibniz Universität Hannover, 30419 Hannover, Germany.
Email: tschowri@ifmb.uni-hannover.de

Funding information
H2020 European Research Council, Grant/Award Number: 864971; Deutsche Forschungsgemeinschaft, Grant/Award Number: TS 325/1-1 and TS 325/2-2

Abstract

The widespread bacterial second messenger bis-(3′-5′)-cyclic diguanosine monophosphate (c-di-GMP) is an important regulator of biofilm formation, virulence and cell differentiation. C-di-GMP-specific biosensors that allow detection and visualization of c-di-GMP levels in living cells are key to our understanding of how c-di-GMP fluctuations drive cellular responses. Here, we describe a novel c-di-GMP biosensor, CensYBL, that is based on c-di-GMP-induced dimerization of the effector protein BldD from *Streptomyces* resulting in bimolecular fluorescence complementation of split-YPet fusion proteins. As a proof-of-principle, we demonstrate that CensYBL is functional in detecting fluctuations in intracellular c-di-GMP levels in the Gram-negative model bacteria *Escherichia coli* and *Salmonella enterica* serovar Typhimurium. Using deletion mutants of c-di-GMP diguanylate cyclases and phosphodiesterases, we show that c-di-GMP dependent dimerization of CBldD-YPet results in fluorescence complementation reflecting intracellular c-di-GMP levels. Overall, we demonstrate that the CensYBL biosensor is a user-friendly and versatile tool that allows to investigate c-di-GMP variations using single-cell and population-wide experimental set-ups.

KEYWORDS
bimolecular fluorescence complementation, biosensor, BldD, c-di-GMP, diguanylate cyclase, EAL, GGDEF, phosphodiesterase

1 | INTRODUCTION

Cyclic dinucleotide second messengers are key components of signal transduction systems for bacterial adaptation to environmental cues. Bis-(3′,5′)-cyclic diguanosine monophosphate (c-di-GMP) was discovered in 1987 as a stimulator of cellulose synthase in *Komagataeibacter xylinus* (Ross et al., 1987) and is now recognized as a conserved central regulator of bacterial physiology (Jenal et al., 2017). Diguanylate cyclases (DGCs) and c-di-GMP-specific phosphodiesterases (PDEs) possess antagonistic activities and control intracellular c-di-GMP levels in response to diverse signals. DGCs synthesize c-di-GMP out of GTP through their catalytic GGDEF domains that are named after key amino acids in their active sites (Paul et al., 2004). c-di-GMP-specific PDEs carry either EAL or HD-GYP domains. EAL-type PDEs hydrolyze c-di-GMP to the linear 5′-phosphoguanylyl-(3′-5′)-guanosine (pGpG) dinucleotide (Christen

Manuel Halte and Mirka E. Wörmann contributed equally to this work.

This is an open access article under the terms of the Creative Commons Attribution-NonCommercial-NoDerivs License, which permits use and distribution in any medium, provided the original work is properly cited, the use is non-commercial and no modifications or adaptations are made.
© 2021 The Authors. *Molecular Microbiology* published by John Wiley & Sons Ltd.

13652958, 2022, 3, Downloaded from https://onlinelibrary.wiley.com/doi/10.1111/mmi.14876 by Humboldt-Universitat Zu Berlin, Wiley Online Library on [28/02/2023]. See the Terms and Conditions (https://onlinelibrary.wiley.com/terms-and-conditions) on Wiley Online Library for rules of use; OA articles are governed by the applicable Creative Commons License

et al., 2005; Schmidt et al., 2005) while HD-GYP domains cleave c-di-GMP to two molecules of GMP (Bellini et al., 2014).

c-di-GMP exerts a global regulatory role on diverse bacterial functions, including biofilm formation, motility, virulence, cell cycle progression and cell differentiation by binding to an array of protein effectors and riboswitches (Chou & Galperin, 2016; Römling et al., 2013). Intracellular levels of the molecule range from nanomolar to low-micromolar concentrations between bacterial species (Abel et al., 2013; Sarenko et al., 2017). Interestingly, c-di-GMP levels can also vary between individual cells of an isogenic population leading to phenotypic diversity, as exemplified by *Salmonella* Typhimurium during infection (Petersen et al., 2019). In *Bacillus subtilis* subpopulations, high c-di-GMP levels correlate with the transition to sporulation, while low levels are associated with competence (Weiss et al., 2019). Moreover, in *Caulobacter crescentus* asymmetrical distribution of c-di-GMP within the cell through local action of c-di-GMP-metabolizing enzymes was reported to be critical for positioning of the polar flagellum (Christen et al., 2010).

Monitoring c-di-GMP patterns in living cells revealed fundamental new insights into c-di-GMP-dependent phenotypic heterogeneity and in vivo functions of DGCs and PDEs. This became only possible by the application of fluorescence-based methods for detection of c-di-GMP in vivo. Three different approaches can be employed for biosensing of the second messenger. First, c-di-GMP-responsive promoters can be fused upstream of the genes encoding fluorescent proteins and used as indirect reporters of the intracellular dinucleotide levels in living cells. For example, a transcriptional fusion of the promoter of the *cdrA* gene, encoding a large adhesin in *Pseudomonas aeruginosa*, to the gene encoding for green fluorescent protein (GFP) revealed that *P. aeruginosa* responds to surface attachment by increased production of c-di-GMP (Rodesney et al., 2017; Rybtke et al., 2012). Second, riboswitches that specifically bind c-di-GMP to their aptamer domains (Sudarsan et al., 2008) can be utilized as c-di-GMP biosensors. Ligand-binding aptamers were successfully fused to RNA aptamers that incorporate small fluorophores like 3,5-difluoro-4-hyd roxybenzylidene imidazolinone (DFHBI) and emit fluorescence. In such riboswitch-based biosensors, binding of c-di-GMP leads to conformational changes in the fused aptamer which results in DFHBI binding and fluorescence that can be monitored to estimate c-di-GMP levels (Kellenberger et al., 2013; Nakayama et al., 2012). Alternatively, c-di-GMP-responsive riboswitches can be fused to fluorescent proteins to detect the second messenger in living cells (Weiss et al., 2019; Zhou et al., 2016). Finally, c-di-GMP-binding proteins can be utilized as biosensors for the dinucleotide. For example, the c-di-GMP effector YcgR from *Salmonella enterica* serovar Typhimurium undergoes a conformational change upon ligand binding which can be coupled to Förster resonance energy transfer (FRET) (Christen et al., 2010; Kulasekara et al., 2013). Recently, as an alternative to fluorescence-based biosensors, a ratiometric biosensor based on bioluminescence resonance energy transfer (BRET) was developed to study bacterial c-di-GMP concentrations (Dippel et al., 2020).

In this study, we describe the development and application of a c-di-GMP biosensor that utilizes bimolecular fluorescence complementation (BiFC) of the yellow fluorescence protein (YPet) upon ligand binding to the c-di-GMP effector BldD. The principle is based on two split non-fluorescent fragments of YPet, which, when brought together by interaction between proteins or proteins domains that are fused to each fragment, undergo fluorescence complementation (Hu et al., 2002). The transcriptional regulator BldD has recently been identified as a c-di-GMP effector in *Streptomyces venezuelae* (Tschowri et al., 2014). During their developmental life cycle, *Streptomyces* undergo a complex physiological and morphological transition that culminates in the formation of dormant spores (Bush et al., 2015). BldD binds a tetrameric c-di-GMP to the RxD-X8-RxxD signature motif in the C-terminal domain of BldD (CBldD), which in turn drives BldD dimerization. Dimerized BldD binds to its target promoters to represses a broad regulon of sporulation genes (den Hengst et al., 2010). Structural and biochemical studies revealed that the $BldD_2$-$(c\text{-}di\text{-}GMP)_4$ complex assembles in an ordered, sequential manner. First, a c-di-GMP dimer binds to BldD motif 2 (RxxD), which induces conformational changes that favor binding of the second dimer to motif 1 (RxD) (Schumacher et al., 2017). Importantly, in the $BldD_2$-$(c\text{-}di\text{-}GMP)_4$ complex, the two CBldDs are separated by about 10 Å and are linked together purely by c-di-GMP that acts as a macromolecular dimerizer. Therefore, c-di-GMP-dependent dimerization of CBldD is ideally suited to be employed for c-di-GMP driven BiFC and thus, for in vivo detection of c-di-GMP. Here, we describe the design and demonstrate successful application of a biosensor based on bimolecular fluorescence complementation of a YPet fusion to the c-di-GMP effector BldD (CensYBL) to quantify and monitor fluctuations in c-di-GMP levels of individual cells and bacterial populations of the model organisms *Escherichia coli* and *S*. Typhimurium.

2 | RESULTS

2.1 | Design and characterization of CensYBL as in vivo c-di-GMP biosensor

Guided by structural and biochemical data revealing that CBldD dimerization is driven purely by c-di-GMP, we sought to design a CBldD-based in vivo sensor for c-di-GMP that utilizes the bimolecular fluorescence complementation principle. The BiFC approach is based on complementation of split fluorophores and is frequently used for the detection of protein–protein interactions (Kerppola, 2009). First, we split the yellow fluorescence protein into two fragments and tested protein–protein interaction-driven fluorescence complementation by using an established two-hybrid interaction (Karimova et al., 1998). For that, the N-terminal fraction of YPet (NYPet), comprising amino acids 1–173, was fused to the dimerizing leucine zipper part (“zip”) domain of the yeast transcription factor GCN4 in the pKT25 vector and the C-terminal part of YPet (CYPet), comprising amino acids 156–239, was fused to the zip

13652958, 2022, 3, Downloaded from https://onlinelibrary.wiley.com/doi/10.1111/mmi.14876 by Humboldt-Universitat Zu Berlin, Wiley Online Library on [28/02/2023]. See the Terms and Conditions (https://onlinelibrary.wiley.com/terms-and-conditions) on Wiley Online Library for rules of use; OA articles are governed by the applicable Creative Commons License

domain in pUT18C. As a control, we designed pKT25 and pUT18C-based vectors expressing either NYPet or CYPet without being fused to the interacting Zip proteins (Figure S1a). As shown in Figure S1b, the expression of NYPet-Zip1 and CYPet-Zip2 in *E. coli* led to a fluorescence YPet signal, while no fluorescence was detectable in cells co-expressing the separated YPet fragments only.

Next, we fused NYPet and CYPet, respectively, to the C-terminal domain of BldD from *S. venezuelae* (CBldD, comprising residues 80–166) including a GSGGG linker between the two domains and cloned the two synthetically generated open reading frames in tandem into the pTrc99a-FFA vector (Amann et al., 1988) (Figure 1a–c). We named the biosensor fusion protein CensYBL for C-di-gmp sENSor Ypet BLdD. For normalization of CensYBL expression between individual cells, we generated a transcriptional fusion of the *mcherry* gene downstream of the CensYBL-encoding genes. As such, in the plasmid pCensYBL, the expression of the three genes *nypet*::*cbldD*, *cypet*::*cbldD*, and *mcherry* is controlled by the same IPTG inducible P*trc* promoter. In line with our expectations, we detected strong YPet and mCherry signals, respectively, upon induction of pCensYBL for 1 hr using 250 μM IPTG in *E. coli* (Figure 2a).

CBldD interacts with c-di-GMP using two adjacent motifs. Motif 1 is composed of residues 114–116 (RxD) and motif 2 comprises residues 125–128 (RxxD) (Figure 1d). Mutagenesis of either motif 1 or motif 2 completely abolishes c-di-GMP-binding (Tschowri et al., 2014). We aimed to design an inactive BldD-based biosensor that is blind for c-di-GMP as a specificity control (CensYBL*). For that, we swapped the arginine residues in motif 1 and 2 with aspartic acid and vice versa as described in Tschowri et al., 2014 leading to CbldD*, which is unable to bind the second messenger. As shown in Figure 2a, the expression of the split YPet fragments fused to CbldD* led to weak background fluorescence only. Altogether, our data demonstrate that c-di-GMP dependent CBldD-dimerization results in functional complementation of NYPet and CYPet and can be utilized as a tool for in vivo detection of c-di-GMP.

Upon confirming successful complementation of split YPet fused to CbldD when expressed from pCensYBL, we assessed the in vivo protein expression levels of CYPet- and NYPet-CbldD and mCherry in *E. coli*-K12 W3110 (Hayashi et al., 2006). Active and inactive form of CensYBL were expressed in strains with modulated levels of c-di-GMP due to overexpression of a PDE ($PdeH^+$) or a DGC ($DgcC^+$) from the IPTG-inducible pCAB18 plasmid (Tschowri et al., 2009). We next performed Western Blot analyses of whole cell lysates using anti-BldD and anti-mCherry antibodies, respectively (Figure S2a). In line with our expectations, no striking differences of NYPet/CYPet-CbldD and mCherry protein levels were observed in the wild-type strain compared to the strains expressing a PDE/DGC, confirming that differences in c-di-GMP levels do not impact the expression of CensYBL and mCherry. Respective loading controls are shown in Figure S2b. However, we detected lower levels of the fusion protein in cells expressing the inactive biosensor CensYBL*. Split YFP were reported to be prone to aggregation when interaction between the split fragments failed (Kostecki et al., 2010). This is also the case for

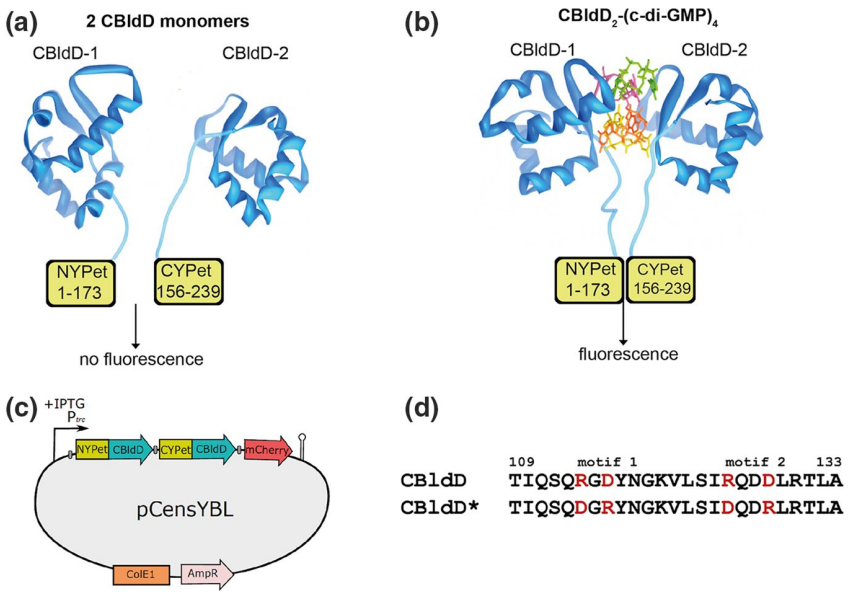

FIGURE 1 Design principle of the CensYBL c-di-GMP biosensor. (a, b) Schematic illustration of the CensYBL c-di-GMP biosensor fusion proteins that consist of either the N-terminal part of YPet (NYPet; amino acids 1–173) or the C-terminal part of YPet (CYPet; amino acids 156–239) connected to the C-terminal c-di-GMP-binding domain of BldD (CBldD). (a) In absence of c-di-GMP, CBldD adopts a monomeric conformation that does not support bimolecular complementation of the split YPet fluorophore. (b) Upon binding of a tetrameric c-di-GMP, BldD dimerizes, which allows complementation of the two YPet fragments leading to a fluorescence signal. (c) The pTrc99a-FFA-based pCensYBL vector harbors a *nypet*::*cbldD*, *cypet*::*cbldD* and *mcherry* operon under the control of the IPTG inducible P*trc* promoter. (d) Protein alignment of a BldD fragment (amino acids 109–133) comprising the c-di-GMP binding motif 1 (RxD) and motif 2 (RxxD) in CBldD that are essential for c-di-GMP binding. The amino acids highlighted in red were mutagenized to DxR and DxxR in CBldD* to abolish c-di-GMP binding

13652958, 2022, 3, Downloaded from https://onlinelibrary.wiley.com/doi/10.1111/mmi.14876 by Humboldt-Universitat Zu Berlin, Wiley Online Library on [28/02/2023]. See the Terms and Conditions (https://onlinelibrary.wiley.com/terms-and-conditions) on Wiley Online Library for rules of use; OA articles are governed by the applicable Creative Commons License

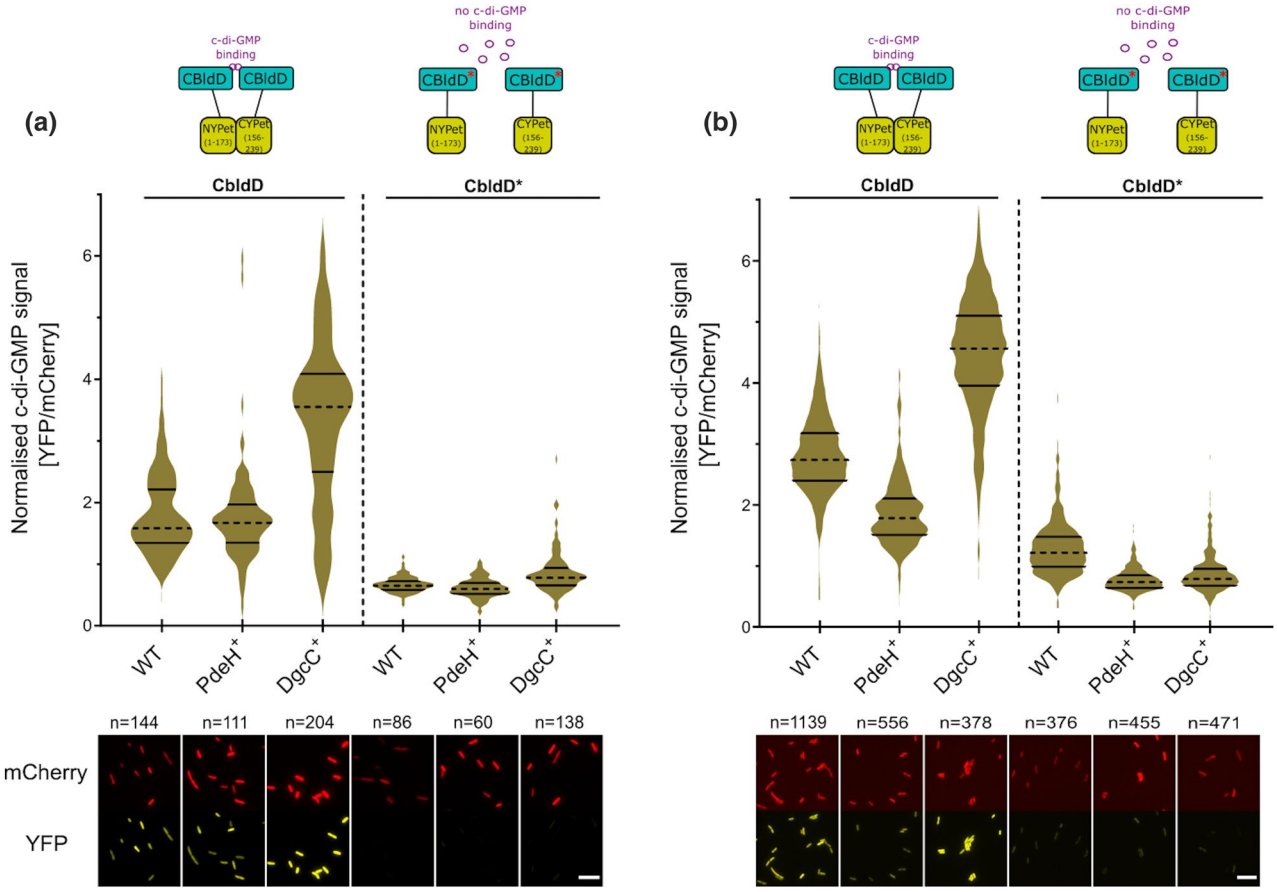

FIGURE 2 The CensYBL biosensor detects changes of intracellular c-di-GMP levels. The active version of the CensYBL biosensor (CbldD) or the inactive version (CbldD*) was used to quantify intracellular c-di-GMP levels in *Escherichia coli* (a) and *S.* Typhimurium (b). Strains overexpressing the PDE PdeH (PdeH$^+$) or the DGC DgcC (DgcC$^+$) were investigated using fluorescence microscopy. The top part of the panels shows violin plots of the normalized c-di-GMP signal obtained from single cell measurements. The dashed lines represent the median and solid lines the quartiles. Representative fluorescent microscopy images of the mCherry and YFP channels are shown in the lower part of the panels. Scale bar = 10 μm

CensYBL* fusions and likely causes protein aggregation or instability. Accordingly, we concluded that the expression of *nypet::cbldD*, *cypet::cbldD* and *mcherry* is independent of the intracellular c-di-GMP levels, and that the observed changes in YPet intensities depend on the intracellular c-di-GMP concentration.

2.2 | CensYBL-based detection of c-di-GMP in individual *E. coli* and *S.* Typhimurium cells

We then aimed to evaluate CensYBL in vivo to monitor intracellular c-di-GMP levels. For this, we used *E. coli* and *S.* Typhimurium strains carrying plasmids overexpressing the PDE PdeH or the DGC DgcC (Pesavento et al., 2008; Richter et al., 2020). Both enzymes are well-characterized and affect c-di-GMP levels in an antagonistic manner. PdeH is a stand-alone EAL domain phosphodiesterase previously known as YhjH in *E. coli* and STM3611 in *S.* Typhimurium (Pesavento et al., 2008). DgcC, formerly designated as YaiC in *E. coli* and STM0385/AdrA in *S.* Typhimurium, is a GGDEF domain DGC. In both species, those enzymes are involved in biofilm regulation by a complex regulatory network controlled by c-di-GMP (Crepin et al., 2017; Kader et al., 2006; Pesavento et al., 2008; Richter et al., 2020). By using those well-characterized enzymes, we aimed to modify the intracellular c-di-GMP levels in order to assess CensYBL sensitivity and its capability to measure different c-di-GMP concentrations on a single-cell level.

Strains harboring plasmids overexpressing PdeH or DgcC under the control of a P*lac* promoter, in combination with plasmids encoding the active or inactive CensYBL biosensor, were grown to exponential phase under IPTG inducing conditions. We then determined the YFP and mCherry fluorescence levels of individual cells using live-cell epi-fluorescence microscopy. The mCherry fluorescence signal was used for normalization of expression, and fluorescence levels of YFP were calculated relative to the mCherry levels for each cell. We found that in the *E. coli* DgcC$^+$ strain, the median c-di-GMP signal (YFP/mCherry fluorescence ratio) was increased by 2-fold (Figure 2a). Contrary to our expectations, the c-di-GMP signal observed in the PdeH$^+$ strain was similar to the wild type. We note, however, that a c-di-GMP concentration of ~60 nM was reported for *E. coli* wild type cells (Sarenko et al., 2017). As the K_D of BldD-CTD for c-di-GMP was determined to be about 2.5 μM (Tschowri et al., 2014), it is possible that we are not able to detect minor differences in intracellular c-di-GMP levels

13652958, 2022, 3, Downloaded from https://onlinelibrary.wiley.com/doi/10.1111/mmi.14876 by Humboldt-Universitat Zu Berlin, Wiley Online Library on [28/02/2023]. See the Terms and Conditions (https://onlinelibrary.wiley.com/terms-and-conditions) on Wiley Online Library for rules of use; OA articles are governed by the applicable Creative Commons License

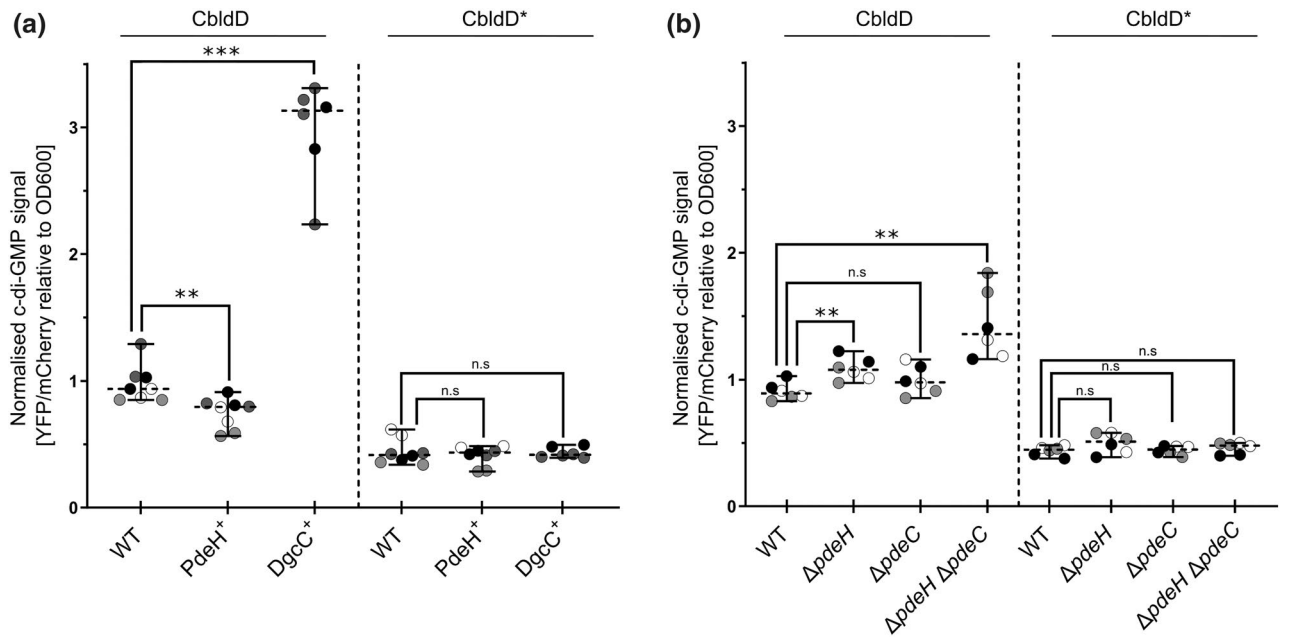

FIGURE 3 The CensYBL c-di-GMP biosensor detects fluctuations in c-di-GMP levels in population measurements. The active version of the CensYBL biosensor (CbldD) or the inactive version (CbldD*) was used to quantify c-di-GMP levels in *S*. Typhimurium using plate reader-based population measurements. (a) C-di-GMP levels were quantified in *S*. Typhimurium strains overexpressing the PDE PdeH (PdeH$^+$) or the DGC DgcC (DgcC$^+$). The dashed lines represent the median of the normalized c-di-GMP signals and the solid lines the 95% CI, obtained from six biological replicates (the mean of each biological replicate was calculated from three technical replicates measurements). Unpaired two-tailed Student's *t*-tests with 95% confidence level were performed (ns: *p*-value > .05, **: *p*-value ≤ .01, ***: *p*-value ≤ .001). (b) C-di-GMP levels were quantified in *S*. Typhimurium PDE deletion strains (Δ*pdeH*/Δ*pdeC*). The dashed lines represent the median of the normalized c-di-GMP signals and the solid lines the 95% CI, obtained from six biological replicates analyzed on three different days (the mean of each biological replicate was calculated from three technical replicates measurements). Unpaired two-tailed Student's t-tests with 95% confidence level were performed (ns: *p*-value > .05, **: *p*-value ≤ .01, ***: *p*-value ≤ .001). The color represents the biological replicates of each day

between the wild type and upon PdeH$^+$ overexpression in *E. coli*. We note that for the CensYBL* mutant biosensor defective in c-di-GMP binding, we observed a background fluorescence signal only in all strains analyzed. In complementing experiments, we next tested the ability of the CensYBL biosensor to monitor intracellular c-di-GMP levels in *S*. Typhimurium strains carrying the same plasmids overexpressing a PdeH or DgcC, together with the active/inactive CensYBL biosensor (Figure 2b). We detected a similar increase of the intracellular c-di-GMP signal in a strain expressing DgcC$^+$ compared to the respective *E. coli* strain. Contrary to our data obtained with *E. coli*, we observed a 1.5-fold decrease in the c-di-GMP signal in the PdeH$^+$ strain compared to wild type. We conclude that CensYBL can detect intracellular differences in c-di-GMP concentrations in Gram-negative bacteria and can be used for functional analysis of DGCs and PDEs in vivo.

2.3 | CensYBL-based detection of c-di-GMP fluctuations in a *S. enterica* population

In addition to quantifying intracellular c-di-GMP levels using microscopy-based single cell analysis, we aimed to determine if the CensYBL biosensor can be used for c-di-GMP detection and quantification using plate reader measurements. Such an approach would be advantageous to facilitate the screening of a large number of mutants in a time-efficient and easy manner. We therefore measured the c-di-GMP signal in *Salmonella* strains overexpressing either DgcC or PdeH as presented above, as well as using mutants deleted either for the PDE-encoding genes *pdeH* or *pdeC* and the Δ*pdeH* Δ*pdeC* double mutant. PdeC (STM4264) is a PDE phosphodiesterase orthologue to *E. coli* YjcC and contains an EAL domain involved in invasion and biofilm formation control in *Salmonella* (Ahmad et al., 2011, 2017).

After induction of CensYBL expression, the cells were collected by centrifugation, washed in PBS and loaded onto 96-well plates. Measured fluorescence values of YFP and mCherry were divided by the OD600, and subsequent YFP/OD600 values were made relative to mCherry/OD600 levels (see Material and Methods). We observed a 0.9-fold decrease and a 3.3-fold increase in the c-di-GMP signals of the PdeH$^+$ and DgcC$^+$ strains (Figure 3a), respectively, similar as observed using the microscopy-based approach. For the single deletion mutants of *pdeH* or *pdeC*, we observed a 1.21 and 1.10-fold increase in the c-di-GMP signals, respectively, while the double deletion mutant (Δ*pdeH* Δ*pdeC*) displayed a 1.5-fold signal increase compared to the wild type (Figure 3b). The inactive CensYBL* biosensor displayed a low signal compared to the active biosensor that was similar between the strains tested. Altogether, our data demonstrate that CensYBL biosensor can be utilized for in vivo detection

13652958, 2022, 3, Downloaded from https://onlinelibrary.wiley.com/doi/10.1111/mmi.14876 by Humboldt-Universitat Zu Berlin, Wiley Online Library on [28/02/2023]. See the Terms and Conditions (https://onlinelibrary.wiley.com/terms-and-conditions) on Wiley Online Library for rules of use; OA articles are governed by the applicable Creative Commons License

and quantification of the intracellular c-di-GMP level of individual bacteria and for screening of c-di-GMP mutants using plate reader measurements.

3 | DISCUSSION

In this work, we developed a novel fluorescent c-di-GMP biosensor, CensYBL, and demonstrate that it can detect fluctuations in intracellular c-di-GMP levels in the Gram-negative species *E. coli* and *S.* Typhimurium. The CensYBL biosensor exploits the mode-of-action of the c-di-GMP binding domain of BldD, a transcriptional regulator that orchestrates the transition from hyphae to spore in *Streptomyces* (Tschowri et al., 2014). BldD forms a homo-dimeric complex, where two BldD monomers dimerize in presence of four c-di-GMP molecules. Hereby, the second messenger specifically interacts with the RxD-X8-RxxD motif in the C-terminal domain of BldD and glues together the otherwise separated BldD monomers. We reasoned that this dimerization mechanism, that is driven exclusively by c-di-GMP, is perfectly suited for utilization as a c-di-GMP sensor system. For the design of such a BldD-based biosensor, we therefore fused the c-di-GMP-sensing domain of BldD to the C-terminal and N-terminal regions of YPet in order to utilize BiFC as readout for c-di-GMP binding. Our data shown in Figures 2 and 3 demonstrate that the CensYBL biosensor is suitable to detect changes in the intracellular c-di-GMP concentration both using fluorescence microscopy at the single cell level, and using plate reader-based population measurements. CensYBL could also be used to investigate spatial localization of c-di-GMP, for example, asymmetrical distribution of the second messenger within individual cells or localized patterns within structured macrocolony biofilms, when combined with colony cryosectioning. Recent developments in photo-activated localization microscopy (PALM) and the necessary photoactivable fluorescent proteins usable for BiFC as well as PALM (Liu et al., 2014; Stockmar et al., 2018), could allow CensYBL-based detection of local c-di-GMP pools within the cytoplasm. Our pTrc99A-FF4 vector-based system could be widely used in *Enterobacteriaceae* species, however, the biosensor-comprising genes could be cloned under the control of an inducible promoter to enable expression in any other vector compatible with the species of interest. Thus, CensYBL has a great potential for versatile applications studying c-di-GMP regulation in a wide range of bacteria.

As a proof-of-principle, we investigated the ability of the CensYBL biosensor to detect differences in intracellular c-di-GMP levels upon overexpression of PDEs and DGCs. Interestingly, we found that the CensYBL biosensor did not detect a lower c-di-GMP signal upon overproduction of PdeH in *E. coli* when compared to the wild-type strain (Figure 2a). The physiological c-di-GMP levels in *E. coli* were previously estimated to range between 40 and 80 nM (0.7–1.4 pmol/mg total cellular protein) (Sarenko et al., 2017) and are likely even lower upon overexpression of PdeH. Since the c-di-GMP binding affinity of BldD has been reported to be ~2.5 μM (Tschowri et al., 2014), we cannot exclude that the low c-di-GMP concentrations in wild type *E. coli* may represent the lower detection limit of the CensYBL biosensor. We note, however, that overproduction of DgcC resulted in a strong increase of the c-di-GMP signal detected by CensYBL (Figure 2a). While biosensors with high affinity for c-di-GMP appear advantageous for usage in bacterial strains or species with intracellular c-di-GMP concentrations in the low nM range, application of CensYBL may be beneficial for c-di-GMP detection in cells containing higher c-di-GMP levels. For example, in *Myxococcus xanthus* c-di-GMP levels reach ~85 pmol/mg total cellular protein, i.e. are about 120-fold higher than in *E. coli* (Skotnicka et al., 2016). Overall, CensYBL represents an important addition to the collection of currently available c-di-GMP-specific biosensors.

A non-active version of our CensYBL, expressing a mutated CBldD* in which the c-di-GMP-binding signature was modified to DxR-X8-DxxR, allowed us to demonstrate that bimolecular fluorescence complementation of our biosensor was specifically dependent on c-di-GMP binding to CBldD. Notably, we observed decreased BldD protein levels in the non-active version of CensYBL* (Figure S2a), which we attributed to the lack of CBldD*-NYPet and CBldD*-CYPet interaction likely leading to protein instability. A similar observation was made by Kostecki et al., while studying the protein–protein interaction of *E. coli* DmsA with its binding partner DmsD, using YPet bimolecular fluorescence complementation (Kostecki et al., 2010).

As the current CensYBL design is based on BldD homo-dimer formation, it is further likely that CBldD-NYPet or CBldD-CYPet dimerize themselves, which would result in non-fluorescent complexes and thus reduce the sensitivity of CensYBL biosensor. We further note that the mechanism if and how the $BldD_2$-$(c\text{-}di\text{-}GMP)_4$ complex or the complemented split-YPet complex dissociate is unknown and therefore the CensBYL biosensor might currently not be ideally suited to monitor transient and dynamic changes of c-di-GMP levels. Accumulation of signal due to a lack of dissociation and degradation of CensYBL might additionally limit the study of dynamic changes in intracellular c-di-GMP levels. CensYBL might therefore be optimized in the future by including a C-terminal degradation tag as a target for tail-specific proteases to prevent accumulation of stable, complemented CensYBL biosensor, similar to the use of unstable GFP variants for investigations of transient changes in gene expression (Andersen et al., 1998).

Over the years, various fluorescence and bioluminescence-based sensors have been developed to detect c-di-GMP levels. Translational fusions of fluorophores to YcgR, a c-di-GMP receptor, were used to detect c-di-GMP binding using FRET microscopy (Christen et al., 2010), a technique that requires a specific expertise. Moreover, FRET microscopy might result in lower fluorescence signals and unwanted cross-talk between the donor and acceptor fluorophore when compared to conventional fluorescent microscopy of a single fluorescent protein. Further, transcriptional fusions of fluorescent proteins to c-di-GMP regulated promoters were used to obtain insights into the mechanism of c-di-GMP regulation of *P. aeruginosa* after surface attachment (Rodesney et al., 2017; Rybtke et al., 2012). However, these transcriptional fusions are species-specific and strictly c-di-GMP dependent

13652958, 2022, 3, Downloaded from https://onlinelibrary.wiley.com/doi/10.1111/mmi.14876 by Humboldt-Universitat Zu Berlin, Wiley Online Library on [28/02/2023]. See the Terms and Conditions (https://onlinelibrary.wiley.com/terms-and-conditions) on Wiley Online Library for rules of use; OA articles are governed by the applicable Creative Commons License

promoters might not be known for a given model organism. Finally, riboswitches that specifically bind c-di-GMP were utilized to detect c-di-GMP levels by fusing RNA aptamers to those structures. Binding of c-di-GMP to the riboswitch results in a conformational change and fluorescence emission after addition of small fluorophores ligands (Kellenberger et al., 2013; Nakayama et al., 2012). Recently, a 3-way split GFP was developed, based on the interaction of *Xanthomonas campestris* proteins PilZ and FimX (Mushnikov et al., 2019). Tripartite split-GFP/YFP have been demonstrated to show less self-assembly as a comparison to 2-split systems, and the system appear as a promising tool for c-di-GMP sensing. However, in comparison to the tripartite system used by Mushnikov et al., our pCensYBL vector comprises the *mcherry* gene controlled by the same inducible promoter as the biosensor genes, which is important for normalization of expression levels.

Altogether, the CensYBL c-di-GMP biosensor reported in this study provides the c-di-GMP field with a user-friendly and sensitive system to measure and quantify intracellular c-di-GMP. CensYBL can be used for single cell microscopy measurement, population plate reader measurements, for screening of new c-di-GMP turnover candidates and/or to measure variation of c-di-GMP in a large number of mutants in a time-efficient manner. We expect that this new tool will greatly facilitate future investigations of the complex regulation and physiological importance of the c-di-GMP second messenger in bacteria.

4 | MATERIAL AND METHODS

4.1 | Bacterial strains, plasmids and oligonucleotides

Strains, plasmids and oligonucleotides used in this study are listed in Table S1. The construction of the plasmids pKT25_*nypet*::*cbldD*/*cbldD** and pUT18C_*cypet*::*cbldD*/*cbldD** is described in the Supplementary Experimental Procedures. The active and inactive versions of CensYBL (pTrc99A-FFA_*ypet*(split)-*cbldD[cbldD*]_mCherry_rrnB*) were generated using Gibson Assembly of two fragments. The pTrc99A-FAA backbone sequence was amplified by inverse PCR using primers MW182/183. The sequence coding for the active and inactive biosensor, respectively, was amplified from plasmids pSS170_Perm*_*ypet*(split)-*cbldD/cbldD*_mCherry_rrnB* (for details see Supplementary Experimental Procedures) using primers MW180/181. pSS09 and pSS88 served as templates for amplification of the coding region of *ypet* and *mcherry*, respectively. The sequence of the active and inactive biosensor can be found in the Data S1.

4.2 | Fluorescence microscopy

Strains harboring the active and inactive version of the biosensor were grown in LB Lysogeny Broth (Lennox) [10 g/L tryptone, 5 g/L yeast extract, 5 g/L NaCl] at 30 or 37°C, respectively for *E. coli* and *S.* Typhimurium, for 45 min before induction with 250 μM IPTG. Cultures growth was resumed for 1 and 2 hr, respectively for *E. coli* and *S.* Typhimurium, cells were harvested, washed in PBS, and applied on 1% agarose pads (Sigma). Slides were imaged using a Zeiss Axio Observer Z1 inverted epifluorescence microscope. Images were acquired at 63× magnification with an Axiocam 506 mono CCD-camera using the Zen 2.6 pro software using the filter sets 46 He (YFP) and 64 He (mCherry) and exposure time of 600 ms (YFP) and 800 ms (mCherry), respectively.

4.3 | Image analysis

Fluorescent microscopy images were processed using Fiji (Schindelin et al., 2012). Fluorescence levels were quantified using Fiji plugin MicrobeJ (Ducret et al., 2016). After segmentation and detection of the cells using phase contrast images, the signal-to-noise ratio of mCherry and YFP was measured directly by MicrobeJ in each cell after detection. The subsequent YFP/mCherry ratio was then manually calculated for each cell. Values obtained were plotted using GraphPad Prism version 9.

4.4 | Plate reader measurements

Cultures were grown and induced as described above for the fluorescence microscopy experiments. After growth, 2 ml cells were collected by centrifugation at 15,000 × *g* and the cell pellet was resuspended in 500 μl PBS. Each well of a black 96-well, clear bottom plate was loaded with 150 μl of resuspended culture (Corning, Product number 3603). Measurements of OD (600 nm) and fluorescence were performed using a TECAN Infinite M200 plate reader (TECAN) using excitation/emission wavelengths of 590/620 nm and 510/540 nm for mCherry and YFP, respectively. For each sample, the measured YFP and mCherry fluorescence signal was normalized to the OD600 signal. The YFP values were then normalized to the mCherry values to report the c-di-GMP signal for each sample and plotted using GraphPad Prism version 9.

ACKNOWLEDGEMENTS

This work was supported in part by the European Research Council (ERC) under the European Union's Horizon 2020 research and innovation program (grant to Marc Erhardt; agreement no. 864971). Research in Natalia Tschowri's lab is funded by the DFG Emmy Noether-Program (TS 325/1-1) and the DFG Priority Program SPP 1879 (TS 325/2-2). We thank Heidi Landmesser and Kristin Funke for expert technical assistance. Open access funding enabled and organized by ProjektDEAL.

CONFLICT OF INTEREST

The authors declare no competing interests.

13652958, 2022, 3, Downloaded from https://onlinelibrary.wiley.com/doi/10.1111/mmi.14876 by Humboldt-Universitat Zu Berlin, Wiley Online Library on [28/02/2023]. See the Terms and Conditions (https://onlinelibrary.wiley.com/terms-and-conditions) on Wiley Online Library for rules of use; OA articles are governed by the applicable Creative Commons License

AUTHOR CONTRIBUTIONS

N.T. and M.E. designed the study. All authors designed and interpreted experiments, which were performed by M.H., M.E.W., and M.B. The figures were made by N.T. and M.H. The paper was written by M.H., M.E. and N.T. with input from the other authors.

DATA AVAILABILITY STATEMENT

The data that support the findings of this study are available from the corresponding author upon reasonable request.

ORCID

Manuel Halte https://orcid.org/0000-0001-9876-7493
Marc Erhardt https://orcid.org/0000-0001-6292-619X
Natalia Tschowri https://orcid.org/0000-0002-4304-1860

REFERENCES

Abel, S., Bucher, T., Nicollier, M., Hug, I., Kaever, V., Wiesch, A.Z. et al. (2013) Bi-modal distribution of the second messenger c-di-GMP controls cell fate and asymmetry during the *Caulobacter* cell cycle. *PLoS Genetics*, *9*, e1003744. https://doi.org/10.1371/journal.pgen.1003744

Ahmad, I., Cimdins, A., Beske, T. & Romling, U. (2017) Detailed analysis of c-di-GMP mediated regulation of *csgD* expression in *Salmonella typhimurium*. *BMC Microbiology*, *17*, 27. https://doi.org/10.1186/s12866-017-0934-5

Ahmad, I., Lamprokostopoulou, A., Le Guyon, S., Streck, E., Barthel, M., Peters, V. et al. (2011) Complex c-di-GMP signaling networks mediate transition between virulence properties and biofilm formation in *Salmonella enterica* serovar Typhimurium. *PLoS One*, *6*, e28351. https://doi.org/10.1371/journal.pone.0028351

Amann, E., Ochs, B. & Abel, K.J. (1988) Tightly regulated *tac* promoter vectors useful for the expression of unfused and fused proteins in *Escherichia coli*. *Gene*, *69*, 301–315. https://doi.org/10.1016/0378-1119(88)90440-4

Andersen, J.B., Sternberg, C., Poulsen, L.K., Bjorn, S.P., Givskov, M. & Molin, S. (1998) New unstable variants of green fluorescent protein for studies of transient gene expression in bacteria. *Applied and Environmental Microbiology*, *64*, 2240–2246. https://doi.org/10.1128/AEM.64.6.2240-2246.1998

Bellini, D., Caly, D.L., McCarthy, Y., Bumann, M., An, S.Q., Dow, J.M. et al. (2014) Crystal structure of an HD-GYP domain cyclic-di-GMP phosphodiesterase reveals an enzyme with a novel trinuclear catalytic iron centre. *Molecular Microbiology*, *91*, 26–38. https://doi.org/10.1111/mmi.12447

Bush, M.J., Tschowri, N., Schlimpert, S., Flärdh, K. & Buttner, M.J. (2015) c-di-GMP signalling and the regulation of developmental transitions in streptomycetes. *Nature Reviews Microbiology*, *13*, 749–760. https://doi.org/10.1038/nrmicro3546

Chou, S.H. & Galperin, M.Y. (2016) Diversity of cyclic di-GMP-binding proteins and mechanisms. *Journal of Bacteriology*, *198*, 32–46. https://doi.org/10.1128/JB.00333-15

Christen, M., Christen, B., Folcher, M., Schauerte, A. & Jenal, U. (2005) Identification and characterization of a cyclic di-GMP-specific phosphodiesterase and its allosteric control by GTP. *The Journal of Biological Chemistry*, *280*, 30829–30837. https://doi.org/10.1074/jbc.M504429200

Christen, M., Kulasekara, H.D., Christen, B., Kulasekara, B.R., Hoffman, L.R. & Miller, S.I. (2010) Asymmetrical distribution of the second messenger c-di-GMP upon bacterial cell division. *Science*, *328*, 1295–1297. https://doi.org/10.1126/science.1188658

Crepin, S., Porcheron, G., Houle, S., Harel, J. & Dozois, C.M. (2017) Altered regulation of the diguanylate cyclase YaiC reduces production of type 1 fimbriae in a Pst mutant of uropathogenic *Escherichia coli* CFT073. *Journal of Bacteriology*, *199*, e00168-17. https://doi.org/10.1128/JB.00168-17

den Hengst, C.D., Tran, N.T., Bibb, M.J., Chandra, G., Leskiw, B.K. & Buttner, M.J. (2010) Genes essential for morphological development and antibiotic production in *Streptomyces coelicolor* are targets of BldD during vegetative growth. *Molecular Microbiology*, *78*, 361–379. https://doi.org/10.1111/j.1365-2958.2010.07338.x

Dippel, A.B., Anderson, W.A., Park, J.H., Yildiz, F.H. & Hammond, M.C. (2020) Development of ratiometric bioluminescent sensors for *in Vivo* detection of bacterial signaling. *ACS Chemical Biology*, *15*, 904–914. https://doi.org/10.1021/acschembio.9b00800

Ducret, A., Quardokus, E.M. & Brun, Y.V. (2016) MicrobeJ, a tool for high throughput bacterial cell detection and quantitative analysis. *Nature Microbiology*, *1*, 16077. https://doi.org/10.1038/nmicrobiol.2016.77

Hayashi, K., Morooka, N., Yamamoto, Y., Fujita, K., Isono, K., Choi, S. et al. (2006) Highly accurate genome sequences of *Escherichia coli* K-12 strains MG1655 and W3110. *Molecular Systems Biology*, *2*, 2006 0007. https://doi.org/10.1038/msb4100049

Hu, C.D., Chinenov, Y. & Kerppola, T.K. (2002) Visualization of interactions among bZIP and Rel family proteins in living cells using bimolecular fluorescence complementation. *Molecular Cell*, *9*, 789–798. https://doi.org/10.1016/S1097-2765(02)00496-3

Jenal, U., Reinders, A. & Lori, C. (2017) Cyclic di-GMP: second messenger extraordinaire. *Nature Reviews Microbiology*, *15*, 271–284. https://doi.org/10.1038/nrmicro.2016.190

Kader, A., Simm, R., Gerstel, U., Morr, M. & Römling, U. (2006) Hierarchical involvement of various GGDEF domain proteins in rdar morphotype development of *Salmonella enterica* serovar Typhimurium. *Molecular Microbiology*, *60*, 602–616. https://doi.org/10.1111/j.1365-2958.2006.05123.x

Karimova, G., Pidoux, J., Ullmann, A. & Ladant, D. (1998) A bacterial two-hybrid system based on a reconstituted signal transduction pathway. *Proceedings of the National Academy of Sciences of the United States of America*, *95*, 5752–5756. https://doi.org/10.1073/pnas.95.10.5752

Kellenberger, C.A., Wilson, S.C., Sales-Lee, J. & Hammond, M.C. (2013) RNA-based fluorescent biosensors for live cell imaging of second messengers cyclic di-GMP and cyclic AMP-GMP. *Journal of the American Chemical Society*, *135*, 4906–4909. https://doi.org/10.1021/ja311960g

Kerppola, T.K. (2009) Visualization of molecular interactions using bimolecular fluorescence complementation analysis: characteristics of protein fragment complementation. *Chemical Society Reviews*, *38*, 2876–2886. https://doi.org/10.1039/b909638h

Kostecki, J.S., Li, H., Turner, R.J. & DeLisa, M.P. (2010) Visualizing interactions along the *Escherichia coli* twin-arginine translocation pathway using protein fragment complementation. *PLoS One*, *5*, e9225. https://doi.org/10.1371/journal.pone.0009225

Kulasekara, B.R., Kamischke, C., Kulasekara, H.D., Christen, M., Wiggins, P.A. & Miller, S.I. (2013) c-di-GMP heterogeneity is generated by the chemotaxis machinery to regulate flagellar motility. *eLife*, *2*, e01402. https://doi.org/10.7554/eLife.01402

Liu, Z., Xing, D., Su, Q.P., Zhu, Y., Zhang, J., Kong, X. et al. (2014) Super-resolution imaging and tracking of protein-protein interactions in sub-diffraction cellular space. *Nature Communications*, *5*, 4443. https://doi.org/10.1038/ncomms5443

Mushnikov, N.V., Fomicheva, A., Gomelsky, M. & Bowman, G.R. (2019) Inducible asymmetric cell division and cell differentiation in a bacterium. *Nature Chemical Biology*, *15*, 925–931. https://doi.org/10.1038/s41589-019-0340-4

Nakayama, S., Luo, Y., Zhou, J., Dayie, T.K. & Sintim, H.O. (2012) Nanomolar fluorescent detection of c-di-GMP using a modular aptamer strategy. *Chemical Communications*, *48*, 9059–9061. https://doi.org/10.1039/c2cc34379g

13652958, 2022, 3, Downloaded from https://onlinelibrary.wiley.com/doi/10.1111/mmi.14876 by Humboldt-Universitat Zu Berlin, Wiley Online Library on [28/02/2023]. See the Terms and Conditions (https://onlinelibrary.wiley.com/terms-and-conditions) on Wiley Online Library for rules of use; OA articles are governed by the applicable Creative Commons License

Paul, R., Weiser, S., Amiot, N.C., Chan, C., Schirmer, T., Giese, B. et al. (2004) Cell cycle-dependent dynamic localization of a bacterial response regulator with a novel di-guanylate cyclase output domain. *Genes and Development*, *18*, 715–727. https://doi.org/10.1101/gad.289504

Pesavento, C., Becker, G., Sommerfeldt, N., Possling, A., Tschowri, N., Mehlis, A. et al. (2008) Inverse regulatory coordination of motility and curli-mediated adhesion in *Escherichia coli*. *Genes and Development*, *22*, 2434–2446. https://doi.org/10.1101/gad.475808

Petersen, E., Mills, E. & Miller, S.I. (2019) Cyclic-di-GMP regulation promotes survival of a slow-replicating subpopulation of intracellular *Salmonella* Typhimurium. *Proceedings of the National Academy of Sciences of the United States of America*, *116*, 6335–6340. https://doi.org/10.1073/pnas.1901051116

Richter, A.M., Possling, A., Malysheva, N., Yousef, K.P., Herbst, S., von Kleist, M. et al. (2020). Local c-di-GMP signaling in the control of synthesis of the *E. coli* biofilm exopolysaccharide pEtN-cellulose. *Journal of Molecular Biology*, *432*, 4576–4595. https://doi.org/10.1016/j.jmb.2020.06.006

Rodesney, C.A., Roman, B., Dhamani, N., Cooley, B.J., Katira, P., Touhami, A. et al. (2017) Mechanosensing of shear by *Pseudomonas aeruginosa* leads to increased levels of the cyclic-di-GMP signal initiating biofilm development. *Proceedings of the National Academy of Sciences of the United States of America*, *114*, 5906–5911. https://doi.org/10.1073/pnas.1703255114

Römling, U., Galperin, M.Y. & Gomelsky, M. (2013) Cyclic di-GMP: the first 25 years of a universal bacterial second messenger. *Microbiology and Molecular Biology Reviews*, *77*, 1–52. https://doi.org/10.1128/MMBR.00043-12

Ross, P., Weinhouse, H., Aloni, Y., Michaeli, D., Weinberger-Ohana, P., Mayer, R. et al. (1987) Regulation of cellulose synthesis in *Acetobacter xylinum* by cyclic diguanylic acid. *Nature*, *325*, 279–281. https://doi.org/10.1038/325279a0

Rybtke, M.T., Borlee, B.R., Murakami, K., Irie, Y., Hentzer, M., Nielsen, T.E. et al. (2012) Fluorescence-based reporter for gauging cyclic di-GMP levels in *Pseudomonas aeruginosa*. *Applied and Environmental Microbiology*, *78*, 5060–5069. https://doi.org/10.1128/AEM.00414-12

Sarenko, O., Klauck, G., Wilke, F.M., Pfiffer, V., Richter, A.M., Herbst, S. et al. (2017). More than enzymes that make or break cyclic Di-GMP-local signaling in the interactome of GGDEF/EAL domain proteins of *Escherichia coli*. *mBio*, *8*, e01639-17. https://doi.org/10.1128/mBio.01639-17

Schindelin, J., Arganda-Carreras, I., Frise, E., Kaynig, V., Longair, M., Pietzsch, T. et al. (2012) Fiji: an open-source platform for biological-image analysis. *Nature Methods*, *9*, 676–682. https://doi.org/10.1038/nmeth.2019

Schmidt, A.J., Ryjenkov, D.A. & Gomelsky, M. (2005) The ubiquitous protein domain EAL is a cyclic diguanylate-specific phosphodiesterase: enzymatically active and inactive EAL domains. *Journal of Bacteriology*, *187*, 4774–4781. https://doi.org/10.1128/JB.187.14.4774-4781.2005

Schumacher, M.A., Zeng, W., Findlay, K.C., Buttner, M.J., Brennan, R.G. & Tschowri, N. (2017) The *Streptomyces* master regulator BldD binds c-di-GMP sequentially to create a functional BldD2-(c-di-GMP)4 complex. *Nucleic Acids Research*, *45*, 6923–6933. https://doi.org/10.1093/nar/gkx287

Skotnicka, D., Smaldone, G.T., Petters, T., Trampari, E., Liang, J., Kaever, V. et al. (2016) A minimal threshold of c-di-GMP is essential for fruiting body formation and sporulation in *Myxococcus xanthus*. *PLoS Genetics*, *12*, e1006080. https://doi.org/10.1371/journal.pgen.1006080

Stockmar, I., Feddersen, H., Cramer, K., Gruber, S., Jung, K., Bramkamp, M. et al. (2018) Optimization of sample preparation and green color imaging using the mNeonGreen fluorescent protein in bacterial cells for photoactivated localization microscopy. *Scientific Reports*, *8*, 10137. https://doi.org/10.1038/s41598-018-28472-0

Sudarsan, N., Lee, E.R., Weinberg, Z., Moy, R.H., Kim, J.N., Link, K.H. et al. (2008) Riboswitches in eubacteria sense the second messenger cyclic di-GMP. *Science*, *321*, 411–413. https://doi.org/10.1126/science.1159519

Tschowri, N., Busse, S. & Hengge, R. (2009) The BLUF-EAL protein YcgF acts as a direct anti-repressor in a blue-light response of *Escherichia coli*. *Genes and Development*, *23*, 522–534. https://doi.org/10.1101/gad.499409

Tschowri, N., Schumacher, M.A., Schlimpert, S., Chinnam, N.B., Findlay, K.C., Brennan, R.G. et al. (2014) Tetrameric c-di-GMP mediates effective transcription factor dimerization to control *Streptomyces* development. *Cell*, *158*, 1136–1147. https://doi.org/10.1016/j.cell.2014.07.022

Weiss, C.A., Hoberg, J.A., Liu, K., Tu, B.P. & Winkler, W.C. (2019) Single-cell microscopy reveals that levels of cyclic di-GMP vary among *Bacillus subtilis* subpopulations. *Journal of Bacteriology*, *201*, e00247-19. https://doi.org/10.1128/JB.00247-19

Zhou, H., Zheng, C., Su, J., Chen, B., Fu, Y., Xie, Y. et al. (2016) Characterization of a natural triple-tandem c-di-GMP riboswitch and application of the riboswitch-based dual-fluorescence reporter. *Scientific Reports*, *6*, 20871. https://doi.org/10.1038/srep20871

SUPPORTING INFORMATION

Additional supporting information may be found in the online version of the article at the publisher's website.

How to cite this article: Halte, M., Wörmann, M.E., Bogisch, M., Erhardt, M. & Tschowri, N. (2022) BldD-based bimolecular fluorescence complementation for in vivo detection of the second messenger cyclic di-GMP. *Molecular Microbiology*, 117, 705–713. https://doi.org/10.1111/mmi.14876

13652958, 2022, 3, Downloaded from https://onlinelibrary.wiley.com/doi/10.1111/mmi.14876 by Humboldt-Universitat Zu Berlin, Wiley Online Library on [28/02/2023]. See the Terms and Conditions (https://onlinelibrary.wiley.com/terms-and-conditions) on Wiley Online Library for rules of use; OA articles are governed by the applicable Creative Commons License